LAWRENCE
LIVERMORE
NATIONAL
LABORATORY

LLNL-CONF-404179

Current understanding of divertor detachment: experiments and modelling

W. Wischmeier, M. Groth, A. Kallenbach, A.V. Chankin, D.P. Coster, R. Dux, A. Herrmann, H.W. Muller, R. Pugno, D. Reiter, A. Scarabosio, J.G. Watkins, The DIII-D Team, ASDEX Upgrade Team

May 27, 2008

18th Conference on Plasma Surface Interactions
Toledo, Spain
May 26, 2008 through May 30, 2008

Disclaimer

Current understanding of divertor detachment: experiments and modelling

M. Wischmeier [a,*], M. Groth [b], A. Kallenbach [a], A. V. Chankin [a], D. P. Coster [a], R. Dux [a], A. Herrmann [a], H. W. Müller [a], R. Pugno [a], D. Reiter [c], A. Scarabosio [a], J G. Watkins [d], DIII-D team and ASDEX Upgrade team

[a] *Max-Planck-Institut für Plasmaphysik, EURATOM-Association, Boltzmannstr. 2, D-85748, Garching, Germany*

[b] *Lawrence Livermore National Laboratory, Livermore, California,USA*

[c] *Institut fuer Plasmaphysik, Euratom Association, Juelich, Germany, Partners in the Trilateral Euregio Cluster*

[d] *Sandia National Laboratory, Albuquerque, NM, USA*

Abstract

A qualitative as well as quantitative evaluation of experimentally observed plasma parameters in the detached regime proves to be difficult for several tokamaks. A series of ohmic discharges have been performed in ASDEX Upgrade and DIII-D at similar as possible plasma parameters and at different line averaged densities, $\bar{n}_e$. The experimental data represent a set of well diagnosed discharges against which numerical simulations are compared. For the numerical modelling the fluid-code B2.5 coupled to the Monte Carlo neutrals transport code EIRENE is used. Only the combined enhancement of effects, such as geometry, drift terms, neutral con-

ductance, increased radial transport and divertor target composition, explains a significant fraction of the experimentally observed asymmetries of the ion fluxes as a function of $\bar{n}_e$ to the inner and outer target plates in ASDEX Upgrade. The relative importance of the mechanisms leading to detachment are different in DIII-D and ASDEX Upgrade.

Key words:

PSI 18 keywords: ASDEX-Upgrade, DIII-D, B2/EIRENE, Edge Modelling, Divertor Plasma

JNM keywords: Divertor Materials, Plasma Material Interaction, Plasma Properties

PACS: 52.20-j, 52.25.Vy, 52.30.Ex, 52.55.Rk, 52.55.Fa

1 Introduction

Modelling of partial detachment during burning plasma operation and design modifications of the divertor structures in ITER rely on 2D fluid-neutrals Monte Carlo codes [1]. The operational window for ITER is limited by an upper upstream separatrix density, n_e^{sep} at which the outer target detaches completely, leading to the density limit. Detachment is defined using the following criteria: The loss of total plasma pressure along a field line between an upstream location above the X-point and the target plate is a necessary condition. The release of potential energy during surface recombination enforces the sufficient condition for detachment, being the reduction of the peak ion

* Max-Planck-Institut für Plasmaphysik, EURATOM-Association, Boltzmannstr. 2, D-85748, Garching, Germany
Email address: marco.wischmeier@ipp.mpg.de (ASDEX Upgrade team).

flux, Γ_t^{pk}, to the target. In the framework established under the International Tokamak Physics Activity (ITPA) Divertor and SOL working group experimental data were taken from lower single null Ohmic and L-mode discharges in ASDEX Upgrade and DIII-D at as similar as possible discharge parameters. The ion ∇B drift was towards the active divertor plates. The discharge parameters cover an ITER relevant SOL collisionality. For ASDEX Upgrade the data compared are taken with graphite (year 2006) and tungsten coated graphite (year 2007) along as divertor target material. In DIII-D all plasma facing components, PFCs, are composed of graphite. In both devices at the lowest $\bar{n}_e$ the inner target is initially partially detached reaching complete detachment with increasing $\bar{n}_e$. The outer target remains attached with increasing peak ion flux density, Γ_{ot}^{pk}, up to a value beyond which detachment occurs, defining the detachment threshold density, $\bar{n}_e^{th}$.

In the past attempts on matching experimental results with experimental data quantitatively and qualitatively at both divertor targets simultaneously has proven to be difficult [2]. The SOLPS5.0 code package [3], using the multi fluid code B2.5 coupled to the neutrals Monte Carlo Code EIRENE (version '99) with the option of activating all drift terms is used. The physics implemented in the code package represents the quantitatively best available representation of our current understanding about the individual processes present in the SOL. By default it includes all deficiencies on the current knowledge of boundary conditions and perpendicular transport.

2 Experiment

Given the definition for detachment the experimental data reported here concentrate on the ion flux densities at the targets, Γ_t. The discharge parameters in ASDEX Upgrade and DIII-D were $I_p = 1.0MA$, $B_T = -2.0T$, $q_{95} \approx 3.4$ with $\sim 210kW$ additional heating power from neutral beam injection in DIII-D. The total power at medium to high $\bar{n}_e$ into the SOL, P_{SOL}, is $\sim 900kW$ for both. In ASDEX Upgrade the cryo pumps were active whereas DIII-D only used the turbo molecular pumps. A more detailed description of the experimental observations in DIII-D and ASDEX Upgrade with the graphite tiles at the target can be found in [4, 5]. The effect of replacing the graphite tiles in the strike point zone by tungsten coated graphite tiles in ASDEX Upgrade was studied in 2007 by producing as similar as possible plasma conditions and strike point as with C tiles. Figure 1 compares the experimental data for the upstream SOL density profiles at 3 different densities with (a) medium to low recycling and $\bar{n}_e \approx 2.6 \times 10^{19} m^{-3}$, (b) at the highest $\bar{n}_e$ prior to detachment and (c) during the detached regime at $\bar{n}_e \approx 6.2 \times 10^{19} m^{-3}$. Detachment occurs between $\bar{n}_e \sim 5.5 \times 10^{19} m^{-3}$ and $\bar{n}_e \sim 6.2 \times 10^{19} m^{-3}$, with an $0.5 \times 10^{19} m^{-3}$ later onset with tungsten coated tiles. At the lowest $\bar{n}_e$ and during detachment Γ_{ot}^{pk} is similar, at the detachment threshold density Γ_{ot}^{pk} is $\sim 30\%$ higher with tungsten coated targets than without. Spectroscopy reveals that volumetric recombination is present during detachment. The absolute value of the total volumetric recombination cannot be determined. Figure 2 shows the experimental inner and outer target profiles from DIII-D for three different $\bar{n}_e$. With increasing $\bar{n}_e$ Γ_{ot}^{pk} initially increases and then decreases. The detachment threshold density is lower in the DIII-D, however the fraction of total radiated

power reaches $\sim 90\%$ whereas it is $\sim 65\%$ in ASDEX Upgrade. In both devices the inner target peak ion flux, Γ_{it}^{pk}, decreases in the strike point region with increasing $\bar{n}_e$ [5]. In ASDEX Upgrade the signals from fixed Langmuir probes in the far SOL indicate a radially increasing Γ_t at high $\bar{n}_e$. Tomographic inversion images of the D_α signal show enhanced radiation in the far SOL close to the target plate, whilst spectroscopic measurements along the inner heat shield show an enhanced atomic influx of the fuel species at high $\bar{n}_e$, Fig 3 a). These data correlate with measurements by a fast pressure gauges in ASDEX Upgrade at the bottom of the inner heat shield [6, 7].

3 Numerical Modelling

The aim of the modelling is to attempt to reproduce qualitatively and quantitatively the behavior of Γ_t simultaneously at the inner and outer targets as a function of $\bar{n}_e$ for ASDEX Upgrade and DIII-D. Similar experimental observations have not been reproduced using coupled $2D$ fluid $3D$ neutrals Monte Carlo codes [8]. The ingredients that can contribute to detachment are thought to be sufficient removal of power resulting in a divertor plasma at low temperature in which charge exchange collisions and volumetric recombination processes can be active in a large enough volume to remove momentum and charges from the plasma volume [3, 9]. In order to provide a wide scan of parameters grids of 48×18 cells have been used for ASDEX Upgrade, fig. 3 b) representing a closed divertor geometry with respect to neutrals, and DIII-D, Fig. 6 a) representing an open divertor geometry, based on the experimental magnetic configurations. Therefore the difference in geometry is taken into account.

3.1 ASDEX Upgrade

A detailed description of the general modelling set up for ASDEX Upgrade that produced a satisfying agreement between modelled data and experimental data at the lowest density $\bar{n}_e \approx 2.6 \times 10^{19} m^{-3}$ can be found in [5]. At $\bar{n}_e \approx 2.6 \times 10^{19} m^{-3}$ P_{SOL} is $\sim 560kW$ and $900kW$ at higher $\bar{n}_e$. Starting from the results for the lowest $\bar{n}_e$, n_e^{sep} has been increased applying a feedback scheme on the gas puff. AFor studying the processes in the divertor, as consequence of the 2-point model [10], n_e^{sep} is fixed using a feedback scheme on the gas puff such. For volumetric processes data from a collision radiative model are used including the possibility of molecular assisted recombination effects (MAR) [11]. By resolving the vibrationally excited levels of deuterium molecules using effective energy levels [12] as in [13] MAR could not be observed. In the modelling both Γ_{ot}^{pk} and Γ_{it}^{pk} increase with rising $\bar{n}_e$. This is *qualitatively* in contradiction to the experimental observations.

In high recycling and detached regimes strong poloidal temperature gradients, ∇T_Θ, are expected. With the ion ∇B drift direction towards the outer target the resulting $\mathbf{E_\Theta} \times \mathbf{B}$ drift velocity drives plasma from the LFS to the HFS in regions of ∇T_Θ. However no decreasing Γ_{it}^{pk} as a function of $\bar{n}_e$ is observed. By default the neutral conductivity below the dome is not limited. At low $\bar{n}_e$ a neutral pressure gauge in the outer divertor target plate, [6], measures a neutral flux by a factor ~ 3 smaller than below the dome. Thus the conductivity for neutrals below the dome is limited and was unknown during the simulations. As a mock up a baffle with a small gap is simulated below the dome to limit the neutrals conductivity and test its implications. Without activated drift terms no improve of the results is seen as expected [14]. With all the

drift terms activated, Fig.4 (a) shows how then Γ_{it}^{pk} does not increase and Fig. 4 (b) shows that $\Gamma_{o}^{pk}t$ is in the ballpark of the experimental data. Including the impurity influx measured from spectroscopy along the inner heat shield as an external impurity source into the model does not decrease Γ_{it}^{pk}. However, the results do not imply that the code package does not model detachment as such. The total pressure loss along a field line between the outer midplane and the inner target can be more than a factor of 10 and despite the increase of $\Gamma_{o}^{pk}t$ the total pressure is reduced. In the modelling the high recycling fluxes along the inner heat shield are absent and a further assumption is introduced. The perpendicular particle diffusion coefficient, $D_{\perp}$, has been increased in the far SOL from $1m^2/s$ to $10m^s/s$ and above. Figure 5 shows the resulting effect. This increase does not affect the profiles along of Γ_t considerably at low n_e^{sep}. At the highest density a tendency towards the experimentally observed increased particle fluxes in the far SOL and a reduced Γ_{it}^{pk} is seen which is not seen on the LFS. Even though the activation of drift terms does reduce Γ_{it}^{pk} furthermore it cannot be shown that such enhanced particle fluxes are absent in the far SOL in the absence of activated drift terms.

3.2 DIII-D

In DIII-D, Fig.6 (a), the estimate is $P_{SOL} \sim 800kW$. Experimentally at the lowest $\bar{n}_e$ the upstream n_e and T_e profiles are similar in DIII-D to ASDEX Upgrade [4]. Consequently the same radial profile for perpendicular transport coefficients as for ASDEX Upgrade are used. However, testing different radial profiles of Ξ_e, Ξ_i and $D_{\perp}$ it was not possible simulataneously match a T_e^{sep}, of $\sim 50eV$ and $n_e^{sep} \approx 0.8 \times 10^{19}m^{-3}$ for given P_{SOL} in the margin of the

experimental error bars, resulting in $T_e^{sep} \approx 60 - 65eV$. The modelling of L-mode discharges for DIII-D may be expected to be simpler because unknown parameters as the sub-dome conductance for neutrals or the effective pumping albedo are eliminated. Instead Fig. 6 (b) illustrates the major discrepancies between the modelling and the experimental data for Γ_t^{pk}. Activated drift terms are less stable for simulations of DIII-D. In the modelling without activated drift terms Γ_{it}^{pk} does not decrease as in experiment and Γ_{ot}^{pk} remains larger than the experimental value for all n_e^{sep}. Experimentally with increasing $\bar{n}_e$ and main chamber wall, MCW, recycling a higher impurity influx is expected from the MCW [15]. In the model only neutrals reaching the MCW sputter and the effect of the impinging ion flux can only be taken into account by increasing Y_{chem} for MCW components. This effect reduces Γ_t^{pk} for higher $\bar{n}_e$, Fig.6, but not sufficiently when comparing with experiment. In the code detachment at the outer target occurs at lower n_e^{sep} than for ASDEX Upgrade, as in experiment. This however might be pure coincidence of the not fully reproduced experimental background plasma.

4 Conclusions

Divertor detachment is accessible using code packages such as SOLPS. However, the experimental in-out asymmetry of Γ_t in ohmic/L-mode discharges as a function of $\bar{n}_e$ is not reproduced even with all drift terms activated. Detachment is quantitatively and qualitatively not understood if common assumptions are made. The additional assumption of a limited neutrals conductivity below the dome combined with activating all drift terms reduces Γ_{ot}^{pk} for high n_e^{sep} into the experimental ballpark without affecting results noticeably at

low n_e^{sep}. Drift effects by themselves seem insufficient to explain the divertor asymmetries even though experimentally a change of ion $\nabla\mathbf{B}$ direction experimentally alters the degree of asymmetry [8, 16]. That perpendicular transport in the far SOL is important for the divertor conditions at the inner target cannot be proven with the model. A grid expanding deeper into the SOL is necessary for such an assessment. Enhanced perpendicular transport may be necessary to understand the low Γ_{it}^{pk} and large recycling fluxes from the lower heat shield. Detachment in DIII-D can be a consequence of impurity influx from the MCW.

5 Acknowledgements

This work was performed with support by the Intra-European fellowship (EURATOM) and the auspices of the U.S. Department of Energy by Lawrence Livermore National Laboratory under Contract DE-AC52-07NA27344 and by Sandia National Laboratory under Contract DE-AC04-94AL85000.

References

[1] ITER Physics Basis. *Nucl. Fusion*, **47**(6):S1–S413, 2007.

[2] Chankin A. V. et al. These proceedings I-15.

[3] Schneider R. et al. *Contributions to Plasma Physics*, **40**:328, 2006.

[4] M. Groth et al. *ECA*, 31F:P1–039, 2007.

[5] M. Wischmeier et al. *Contributions to Plasma Physics*, **48**(1-3):249, 2008.

[6] Scarabosio. A et al. These proceedings P2-25.

[7] McCormik K. et al. These proceedings P1-27.

[8] A. Huber et al. *Journal of Nuclear Materials*, **337-339**:241, 2005.

[9] S. I. Krasheninnikov et al. *Physics Letters A*, **214**:285, 1996.

[10] M. Keilhacker et al. *Plasma Physics and Controlled Nuclear Fusion Research*, **III**:183, 1982. Vienna:IAEA.

[11] S. I. Krasheninnikov et al. *Phys. Plasmas*, **4**(5):1638, 1997.

[12] M. Wischmeier et al. *Contributions to Plasma Physics*, **44**(1-3):268, 2004.

[13] U. Fantz et al. *Journal of Nuclear Materials*, **290-293**:367, 2001.

[14] E. Tsitrone et al. *Contributions to Plasma Physics*, **44**(1-3):241, 2004.

[15] D. G. Whyte et al. *Nucl. Fusion*, **41**:1243, 2001.

[16] R. Pitts et al. *Journal of Nuclear Materials*, **337-339**:146, 2005.

6 Figure captions

Fig. 1. Upstream density profiles (top row) and corresponding ion saturation flux profiles (bottom row) at the outer target at three $\bar{n}_e$ in ASDEX Upgrade, comparing cases with C tiles (red) to cases with W coated tiles (black).

Fig. 2.

Ion saturation current profiles along the inner (a) and outer targets (b) of DIII-D at three different $\bar{n}_e$ (red $\bar{n}_e \approx 2.6 \times 10^{19} m^{-3}$, black $\bar{n}_e \approx 3.0 \times 10^{19} m^{-3}$, blue $\bar{n}_e \approx 3.9 \times 10^{19} m^{-3}$.

Fig. 3. Computational grid for ASDEX Upgrade (a) and integral particle D and C influx from the inner lower heat shield of ASDEX Upgrade as a function of $\bar{n}_e$.

Fig. 4. Simulated Γ_t^{pk} showing the effect of reduced neutral conduction with a mock up baffle and the ffect of drifts (a) and comparison with experiment (b) including drifts with $P_{SOL} = 560kW$ at lowest $\bar{n}_e$ and $900kW$ at higher $\bar{n_e}$.

Fig. 5. Radial ion flux profiles at the inner target with and without increased SOL transport.

Fig. 6. Computational grid for DIII-D (a) and comparison of experimental and simulated peak ion fluxes using $Y_{chem} = 1\%$, 2% and $Y_{chem} = 10\%$ from the MCW as a function of n_e^{sep} for DIII-D.

7 Figures

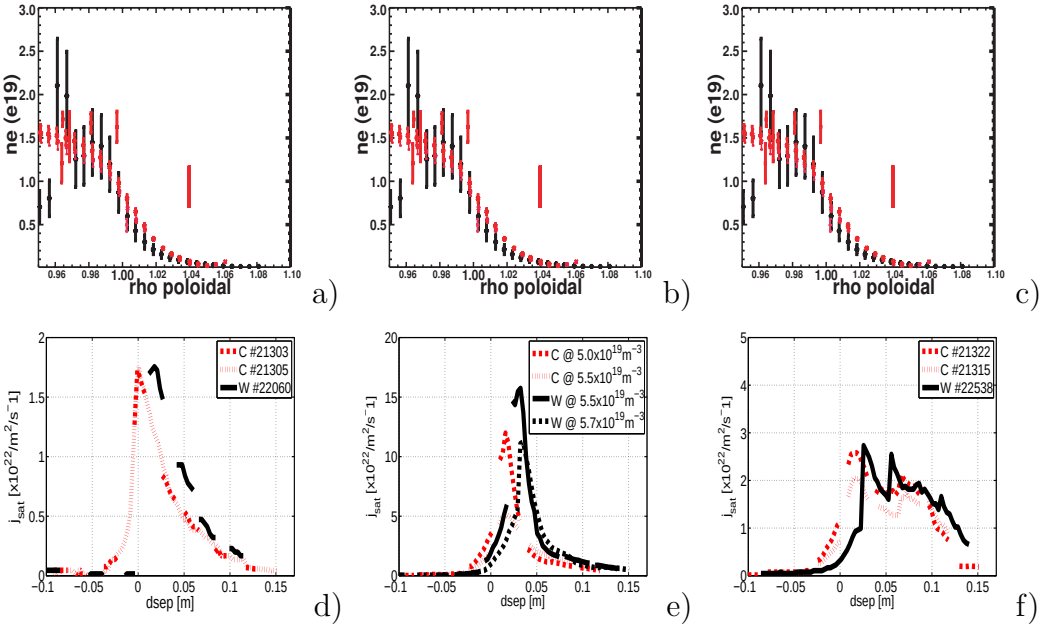

Figure 1

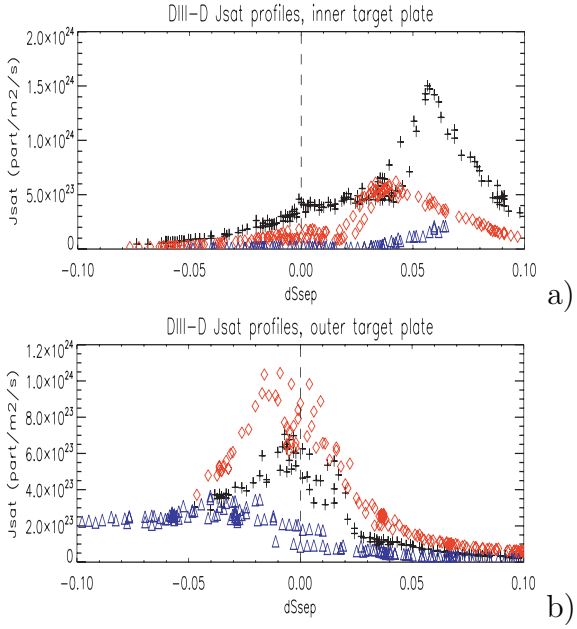

Figure 2

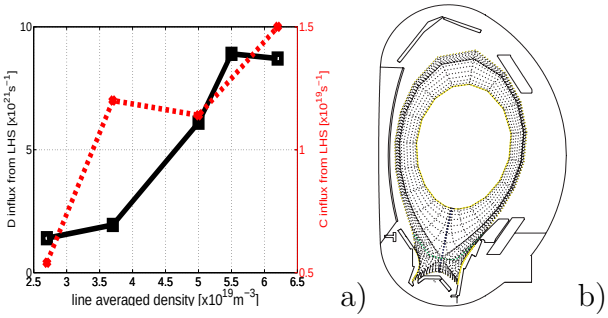

Figure 3

a)

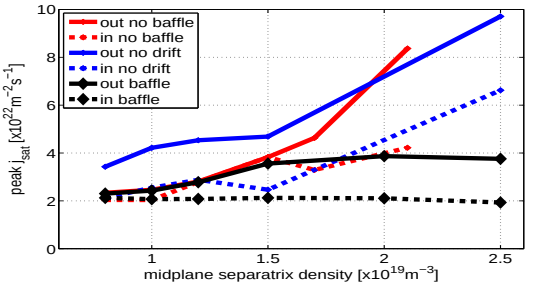

b)

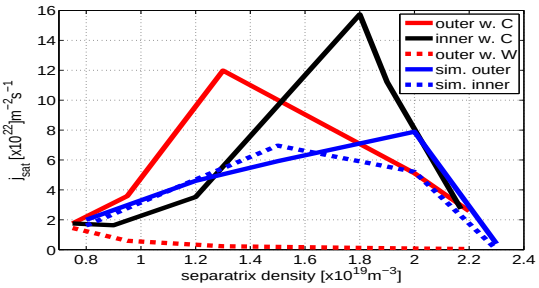

Figure 4

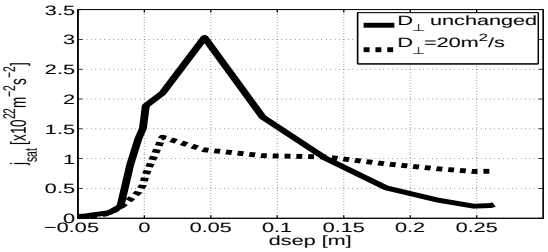

Figure 5

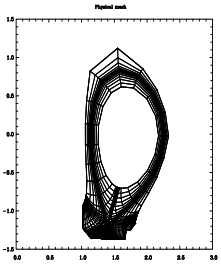

a)

b)

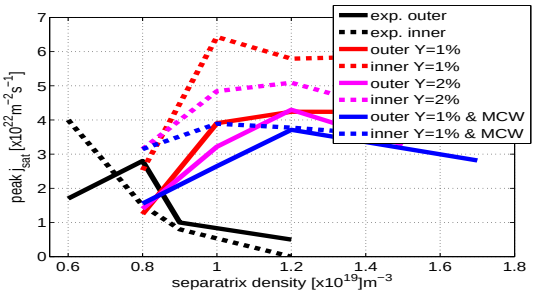
exp. outer
exp. inner
outer Y=1%
inner Y=1%
outer Y=2%
inner Y=2%
outer Y=1% & MCW
inner Y=1% & MCW
peak j_{sat} [x10^{22}m^{-2}s^{-1}]
separatrix density [x10^{19}]m^{-3}
0
1
2
3
4
5
6
7
0.6
0.8
1
1.2
1.4
1.6
1.8

Figure 6